Advances in Computer Science Research, volume 91

International Conference on Modeling, Simulation and Big Data Analysis (MSBDA 2019)

A Sensorless Vector Control Scheme with High Bandwidth Current Loop for Surface Mounted Permanent Magnet Synchronous Machine Based on High Frequency Square Wave Type Voltage Injection

Jinbo Liu[1,*], Jinlei Chen[2] and Fanghong Gao[1]

[1]School of Control Science & Their Engineering, Shandong University, Jinan, P.R.China

[2]Department of Integrated Renewable Energy, School of Engineering, Cardiff University, Cardiff, U.K

*Corresponding author

Keywords: Surfaced-mounted permanent magnet synchronous motor, Sensorless vector control system, High frequency square wave voltage injection, Rotor position observer, Stator flux observer, High bandwidth current loop.

Abstract. Thanks to stator flux based observer running at middle and high speed and various high frequency injection (HFI) methods operating in zero and low speed region, position sensorless field oriented vector control system of permanent-magnet synchronous machine (PMSM) has attracted much attention. Nowadays, Most of HFI methods adopt sinusoidal type voltage at high frequency as injection signal, its frequency being one-tenth of PWM switching frequency or so. Restricted by low pass filters (LPFs) and/or band pass filters (BPFs) used, the control system is implemented with narrow current loop bandwidth and high-frequency audible noise. In order to solve these problems, this paper proposes a new HFI method based on square wave, with its injection frequency equivalent to PWM switching one. Also LPFs and BPFs are replaced with a new demodulation method and then rotor position and velocity can be estimated with rotor position observer. To validate the proposed scheme, a prototype is designed with DSP-TMS320F28335. Whole control system has been designed including initial rotor position determination, magnetic polarity judgment and rotor position and speed estimation by the proposed HFI scheme in low-speed region. Experiments show that the proposed schemes are of good dynamic performance and no additional audible noise is added, its bandwidth of current loop being 500Hz, which approach to that of vector control system of PMSM with encoder.

Introduction

Information of rotor position plays very important part in high-performance servo drive system of PMSM. It can be measured directly from encoder or resolver, or obtained indirectly from estimation methods by means of voltages and currents measured from endpoints of PMSM. Among these sensorless methods, various observer based strategies and high frequency injection (HFI) based methods attract more attention during last two decades, particular the later [1-6]. In principle, observer strategies for rotor position estimation is based on the magnitude of electro-magnetic-force (EMF) at stator, therefore these strategies are only adaptable at high and middle speed. Various HFI methods provide a good means to obtain rotor position and speed at low or even zero speed. They employ constructional asymmetry of rotor, or magnetic asymmetry stimulated by high frequency injection signals to get information of rotor position and speed. So far, according to waveform of which high frequency is injected, these methods can be divided into two types: one is sinusoidal HFI method, the other being square wave HFI one. Usually, the sinusoidal HFI method is more often utilized than later. For sinusoidal HFI method, the signal frequency of which is about one-tenth of PWM switching frequency. Restricted by low pass filters (LPFs) and/or band pass filters (BPFs) used, the control system is only implemented with narrow current loop bandwidth and high-frequency audible noise [7-12].

In order to solve these problems, this paper presents a square wave based HFI scheme, the frequency of which being equal to the PWM frequency. Combined a new demodulation method

with “double sampling and double updating” strategies, the LPFs and BPFs used in sinusoidal HFI method is omitted. Therefore, a high bandwidth current loop and lower audio noise scheme is obtained, the bandwidth of current loop and noise level of which remains the same as that with no HFI signal being injected. To validate the proposed scheme, a prototype is designed. The whole control system is realized including initial rotor position determination, magnetic polarity judgment and rotor position and speed estimation by the proposed HFI scheme in low-speed region.

Fundamental and High-Frequency Mathematical Model of SPMSM

PMSM can be expressed at dq synchronous coordinate reference oriented to rotor in complex vector form as: [16]

$$\vec{u}_{dq} = R_s \vec{i}_{dq} + (D + j\omega_r)\vec{\Psi}_s \tag{1}$$

where $\vec{u}_{dq}$, $\vec{i}_{dq}$ and $\vec{\Psi}_s$ are phase voltage vector $\vec{u}_{dq} = u_d + ju_q$, phase current vector $\vec{i}_{dq} = i_d + ji_q$ and stator flux vector $\vec{\Psi}_s = \Psi_d + j\Psi_q$, respectively. $D = d/dt$, R_s and ω_r are differential operator, stator resistor and rotor angular velocity, respectively.

Neglecting coupling effect between d and q axis, stator flux vector can be represented as

$$\vec{\Psi}_s = L_0 \vec{i}_{dq} + L_1 \vec{i}_{dq}^{*} + \vec{\Psi}_f \tag{2}$$

Where $L_0 = (L_d + L_q)/2$, $L_1 = (L_d - L_q)/2$ are average and differential stator inductance at *dq* synchronous coordinate reference oriented to rotor, respectively. $\vec{\Psi}_f$ is rotor flux vector of magnet, * represents complex conjugation operator, $\vec{i}_{dq}^{*} = i_d - ji_q$. It is worthy to note that L_d is equal to L_q, i.e. $L_d = L_q$ for SPMSM with only fundamental component voltage (without high-frequency signal injection) applied. When an external high-frequency signal is injected into the stator, its inductance may vary due to magnetic saturation under effect of the injected current. As a result, the stator inductances become $L_d \neq L_q$. For this reason, the mathematical model of SPMSM is adjusted to the one which is similar to IPMSM in this paper.

Substituted (2) to (1), we have

$$\begin{aligned} \vec{u}_{dq} &= R_s \vec{i}_{dq} + L_0 D\vec{i}_{dq} + L_1 D\vec{i}_{dq}^{*} \\ &+ j\omega_r (L_0 \vec{i}_{dq} + L_1 \vec{i}_{dq}^{*} + \vec{\Psi}_f) \end{aligned} \tag{3}$$

Under the consideration that the injected high-frequency signal becomes active only at low-speed or near zero speed range, compared with the injected voltage, voltages related to stator resistor and electromagnetic motive force can be neglected. Then the mathematical model at high-frequency can be written from (3) as

$$\vec{u}_{dq} = L_0 D\vec{i}_{dq} + L_1 D\vec{i}_{dq}^{*} \tag{4}$$

Signals in high-frequency square-wave scheme are usually injected into the estimated synchronous coordinate frame $\hat{d}\hat{q}$, not into the real ones dq. The relationship among real dq, the estimated $\hat{d}\hat{q}$ and $\alpha\beta$ at stator coordinate reference can be shown in Fig.1.

In Fig.1, the difference between the estimated rotor position and the real one is defined as

$$\tilde{\theta}_r = \theta_r - \hat{\theta}_r \tag{5}$$

Then

$$\vec{u}_{dq} = e^{-j\tilde{\theta}_r}\vec{u}^{e}_{dq} \tag{6}$$

Substituting (6) into (4), we get

$$\vec{u}^{e}_{dq} = L_0 D\vec{i}^{e}_{dq} + L_1 e^{j2\tilde{\theta}_r} D\vec{i}^{e*}_{dq} \tag{7}$$

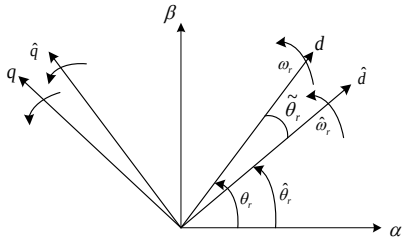

Figure 1. Various reference frames for HF square-wave injection scheme

In order to decrease the effect of injected high-frequency voltage on electromagnetic torque, the voltage is usually injected into $\hat{d}$-axis, thus the high-frequency square-wave voltage is represented as

$$\vec{u}^{e}_{dq} = \vec{u}^{e}_{h} = u_{inj} \tag{8}$$

From (7), the differential value of the high-frequency currents is given as

$$\Delta\vec{i}^{e}_{dq} = \begin{bmatrix}\Delta i^{e}_{d}\\ \Delta i^{e}_{q}\end{bmatrix} = \frac{u_{inj}T_{update}}{(L_0^2 - L_1^2)}\begin{bmatrix}L_0 - L_1\cos 2\tilde{\theta}_r\\ -L_1\sin 2\tilde{\theta}_r\end{bmatrix} \tag{9}$$

Where T_{update} is updated period.

If the differential value of the q-axis current could be adjusted to ensure $\Delta i^{e}_{q} \to 0$ by means of rotor-position-tracking observer or by phase locked loop (PLL), the estimated rotor position $\hat{\theta}_r$ and rotor angular speed $\hat{\omega}_r$ can then be obtained.

Proposed Injection Scheme and Rotor Position Estimator

Proposed Injection Scheme of High-frequency Pulsated Square-wave and Demodulation Method for Fundamental and High-frequency Current Components

Inject high-frequency voltage in square waveform with its expression given from (8) into $\hat{d}$-axis. Then the differential value of currents response at high-frequency between adjacent updated periods can be calculated by (9). However, there may be some problems in practical application given as follows:

- Voltage deformation exists resulting from dead zone behavior during switching between upper leg and lower leg of the inverter, resulting in 6-times pulsation in the differential value of currents.
- Voltage drop due to conduction of switching devices in the inverter and variation of voltage at DC link may have influence on accuracy of the estimated rotor position to some extent.
- Harmonic component from SVPWM modulation may have effect on the differential value of high-frequency current.

The final results due to all of aforementioned factors are that there exist errors for the estimated rotor position. To cope with these problems, this paper adopts a new demodulation scheme, by which the rotor position can be estimated with two subtraction of successive value of differential value of current [12]. Different from [12], this paper utilizes a high-frequency injection method of square waveform, with its frequency being equal to that of switching components. Also, a scheme named

"double sampling and double updating" is adopted. Based on these procedures, this paper proposed a series of optimal solutions including schemes of rotor position updating at differential phases, demodulation of fundamental component of stator current, calculation of rotor position tracking observer with PLL, updating of current loop, et al. Now they are explained as follows:

When the fundamental currents and high-frequency injection voltage are incorporated and applied to the stator winding of PMSM through inverter, the waveform of total stator currents, fundamental currents and high-frequency currents during one PWM switching period are drawn, respectively, in Fig. 2.

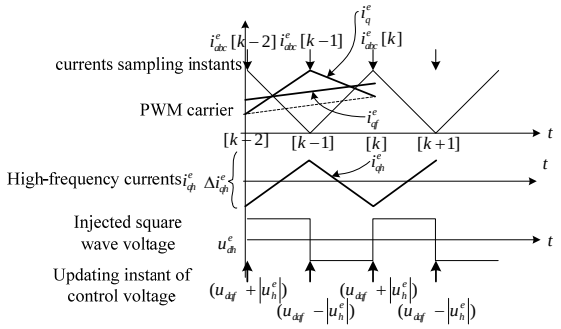

Figure 2. HF square-wave voltage injection scheme and its Implementation

Fig. 2 also shows triangular carrier, High-frequency injection square waveform voltage and its sampling instant and updating instant of applied external control voltage adopted by the proposed scheme. Within each PWM period, currents are sampled twice, and control voltages are updated twice. The injected high-frequency square waveform voltages can be represented as

$$\vec{u}_h^e = u_{dh}^e + ju_{qh}^e = u_{inj} + j0 \tag{10}$$

In order to solve aforementioned problem, subtraction between two successive values of differential value of stator currents are used for the estimation of rotor position angle. Its theoretical derivation is given as follows:

The differential value of currents between *(k-2)* and instant *(k-1)* can be calculated from (9) as

$$\Delta\vec{i}_{dqP}^{\,e} = \begin{bmatrix} \Delta i_{dP}^e \\ \Delta i_{qP}^e \end{bmatrix} = \vec{i}_{dq[k-1]}^{\,e} - \vec{i}_{dq[k-2]}^{\,e} = \frac{u_{inj}T_{update}}{(L_0^2 - L_1^2)} \begin{bmatrix} L_0 - L_1\cos 2\tilde{\theta}_r \\ -L_1 \sin 2\tilde{\theta}_r \end{bmatrix} \tag{11}$$

The differential value of currents between *(k-1)* and instant *k* can be calculated as

$$\Delta\vec{i}_{dqN}^{\,e} = \begin{bmatrix} \Delta i_{dN}^e \\ \Delta i_{qN}^e \end{bmatrix} = \vec{i}_{dq[k]}^{\,e} - \vec{i}_{dq[k-1]}^{\,e}$$
$$= \frac{-u_{inj}T_{update}}{(L_0^2 - L_1^2)} \begin{bmatrix} L_0 - L_1\cos 2\tilde{\theta}_r \\ -L_1 \sin 2\tilde{\theta}_r \end{bmatrix} \tag{12}$$

Subtract (11) from (12), we have

$$\Delta(\Delta\vec{i}_{dqPN}^{\,e}) = \begin{bmatrix} \Delta(\Delta i_{dPN}^e) \\ \Delta(\Delta i_{qPN}^e) \end{bmatrix} = \Delta\vec{i}_{dqP}^{\,e} - \Delta\vec{i}_{dqN}^{\,e}$$
$$= \frac{2u_{inj}T_{update}}{(L_0^2 - L_1^2)} \begin{bmatrix} L_0 - L_1\cos 2\tilde{\theta}_r \\ -L_1 \sin 2\tilde{\theta}_r \end{bmatrix} \qquad = K \begin{bmatrix} \frac{L_0}{L_1} - \cos m\tilde{\theta}_r \\ \sin m\tilde{\theta}_r \end{bmatrix} \tag{13}$$

where m=2,

$$K = \frac{2u_{inj}T_{update}L_1}{(L_0^2 - L_1^2)}$$

The total voltage applied to the stator windings by inverter is

$$\vec{u}_{dq}^{\,e} = \vec{u}_{FOC}^{\,e} + \vec{u}_h^{\,e} \tag{14}$$

Where $\vec{u}_{FOC}^{\,e}$ is the ideal fundamental voltage from current controller, with no connection with nonlinear factors of inverter such as dead-zone, et al. Considering that T_{update} is so short that fundamental voltage remains almost constant. Thus, not only the fundamental currents are deducted by means of subtraction of twice differential value of stator currents, but also the influence due to voltage fluctuation across DC link, low order harmonic voltage are cancelled. The final result of current subtraction is only related to high-frequency square waveform injected voltage (see (13)).

Let $\tilde{\theta}_r \to 0$, then the second equation in (13) becomes

$$\tilde{\theta}_r \approx -\frac{1}{mK}\Delta(\Delta i_{qPN}^{e}) \tag{15}$$

Equation (15) shows that the estimated error of rotor position can be obtained by $\Delta(\Delta i_{qPN}^{e})$. And $\tilde{\theta}_r \to 0$ can be ensured and rotor position angle and angular speed can be available by means of PLL. The fundamental current used for feedback is still sampled at the volley points to eliminate high-frequency disturbance. From Fig.2, the fundamental current is

$$\vec{i}_{dqf}^{\,e} = \vec{i}_{dq[k-1]}^{\,e} - \frac{\Delta(\Delta\vec{i}_{dqPN}^{\,e})}{4} \tag{16}$$

Design of Rotor Position tracking Observer

In order to ensure $\tilde{\theta}_r \to 0$, based PLL rotor position and angular speed tracking observer is adopted, its block diagram is depicted in Fig.3.

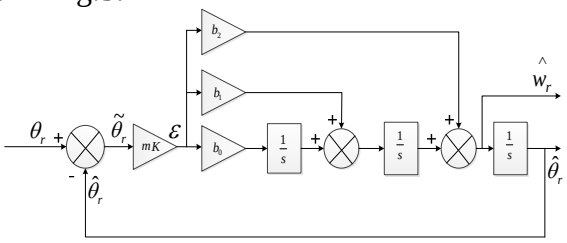

Figure 3. Tracking observer for rotor position and velocity estimation

From Fig.3, the closed-loop transform function of the tracking observer is represented as

$$\frac{\hat{\theta}_r(s)}{\theta_r(s)} = \frac{mK(b_2 s^2 + b_1 s + b_0)}{s^3 + mK(b_2 s^2 + b_1 s + b_0)} \tag{17}$$

If the desired cut-off frequency and damping coefficient is taken as ω_{nd}, ξ_d, respectively, then coefficients of the tracking observer are selected according to (18)

$$\begin{cases} b_0 = \omega_{nd}^3 / mK \\ b_1 = 3\omega_{nd}^2 / mK \\ b_2 = 3\omega_{nd} / mK \end{cases} \tag{18}$$

Fig.4 is the block diagram to fulfill the proposed scheme.

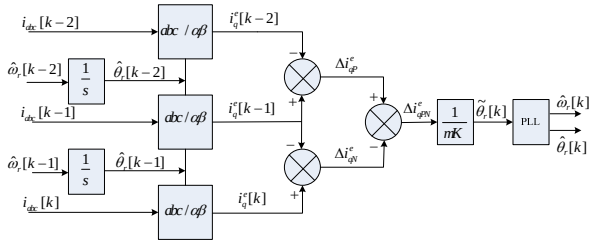

Figure 4. Implementation of the proposed scheme for signals processing and demodulation

High-frequency Square Waveform Voltage Injection Based Sensorless Velocity Control Strategy

The proposed sensorless velocity control system is realized based on field oriented control (FOC), as shown in Fig5.

From Fig.5 we can see the output of speed regulator is taken as desired q-axis current i_q^* , the desired d-axis current is set as $i_d^* = 0$ to obtain maximum torque per ampere (MTPA) control for PMSM. When the high-frequency pulsating square waveform voltage is injected into d-axis, it takes action added with the output of d-axis current controller as the desired d-axis voltage, whereas the output of q-axis current controller is utilized as the desired q-axis voltage. After transformation from dq to $\alpha\beta$ and application of normal seven-sections SVPWM to the inverter, the three-phase currents are produced and measured by two Hall sensors. In turn, the measured three-phase currents are transformed from *abc* to *dq* reference frame and then processed. The rotor position and speed can then be estimated by the proposed scheme with rotor tracking observer.

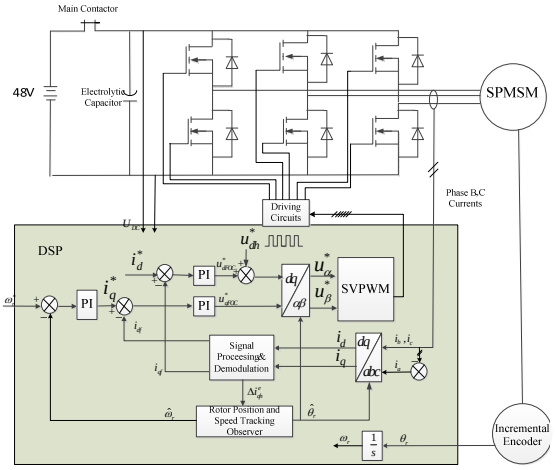

Figure 5. Block diagram of HF square-wave voltage injection based sensorless FOC control system on of PMSM

To ensure realization of whole system illustrated in Fig.5, all parts should be calculated and updated in some sequences. Fig.6 illustrates these sequences and processes including PLL calculation, fundamental and high-frequency current computation and updating of speed-loop, et al., in the proposed scheme.

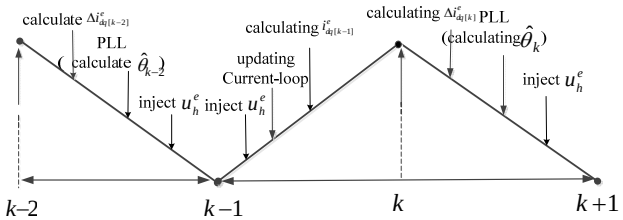

Figure 6. Specific procedures for the proposed scheme

Experimental Results

In order to validate effectiveness of the proposed scheme, a specialized designed prototype of whole control system is manufactured using DSP-TMS320F28335 and also a test platform is built, as shown in Fig.7. A commercial AC PMSM servo motor manufactured by Tamagawa Seiki Co.,LTD is chosen as the tested machine. Its rated values, constructional parameters of the motor, parameters of controllers and tracking observer are given in Table 1. A 750W PMSM servo machine is used as the mechanical load. An incremental encoder with 2000 ppr is installed at its shaft for comparison purpose. MOSFETs with type being IRFS4310Z are selected as switching component for the inverter. Its switching frequency is 10 kHz. Frequency of the injected high-frequency square waveform voltage is also selected at 10KHz, similar to the switching frequency, with its amplitude being 4V. The currents are sampled and the current-loop is updated at the same frequency 20KHz. Voltage across the DC bus is 48V. All the variables in the program are outputted through 12 bits DAC and their waveforms can be observed by oscilloscope. Considering that the rotor position and speed the proposed scheme are estimated from information including $2\tilde{\theta}_r$, the N, S polarities of the rotor PM must be judged firstly at the initial processing program. Thus, to start the motor, three procedures are necessary, i.e., “initial positioning-polarity judgment-initial starting” [10-12].

Figure 7. Platform of sensorless control system of SPMSM

Table 1. Rated values of motor and system parameters

Rated Value	Values	Parameters	Values
Rated Voltage	48V	Stator resistor Per Phase	0.2_{Ω}
Rated Power	200 W	d-axis Inductance	0.57 mH
Rated Velocity	3000 rpm	q-axis Inductance	0.57 mH
Rated Torque	0.43Nm	PM Flux	0.0138 Wb
Pole Pairs	4	Rotational Inertia	$200_{g \cdot cm^2}$
Encoder Pulses	2000 ppr	Proportional Paremeter of Speed Controller Kps	0.03
Proportional Paremeter of d-axis Current Controller Kpid	3.22	Integral Paremeter of Speed Controller Kis	0.0001
Integral Paremeter of d-axis Current Controller Kiid	0.288	Parameter of Position Tracking Observer b0	0.25
Proportional Paremeter of q-axis Current Controller Kpiq	3.22	Parameter of Position Tracking Observer b1	15
Integral Paremeter of q-axis Current Controller Kiiq	0.288	Parameter of Position Tracking Observer b2	1

It is worth noting that during the above “polarity judgment”, the positive and negative pulsated voltages are injected into $\hat{d}$-axis. And the rotor should be remained standstill and the pulsated voltage should be kept active longer than the time constant of d-axis. For the sake of reliability, judgments are repeated for 3 times (see A–phase current in Fig.12 or Fig.13).

In order to verify the performance of current-loop and, a method similar to [10] is used. Mechanical load is applied through the PMSM mechanical load and keep the tested prototype at standstill. Under this condition, a sinusoidal voltage is taken as the desired d-axis current, with its amplitude being 1A, frequency being 500Hz. Fig.8 shows the corresponding waveforms. From top to bottom in Fig.8, the waveforms represent rotor position, the desired d-axis current, the actual one and the actual A-phase current. Fig.9 is its counterpart of Fig.8 for q-axis. From Fig.8 and Fig.9 we can see that the bandwidth of current-loop, whether it is for d-axis or for q-axis, is larger than 500Hz.

Fig.10 also gives waveforms under condition that the desired positive and negative square-wave d-axis currents are switched from each other for further verification of bandwidth of current-loop and dynamic performance, each running for 2s. Definition of waveforms from top to bottom in Fig.10 is the same as Fig.8. Fig.11 shows waveforms under load condition, with the desired speed being +100 rpm and -100rpm, respectively. And they are switched from each other. The definition of waveforms from top to bottom in Fig.11 is the real rotor position from encoder, the estimated rotor position from tracking observer and A-phase current.

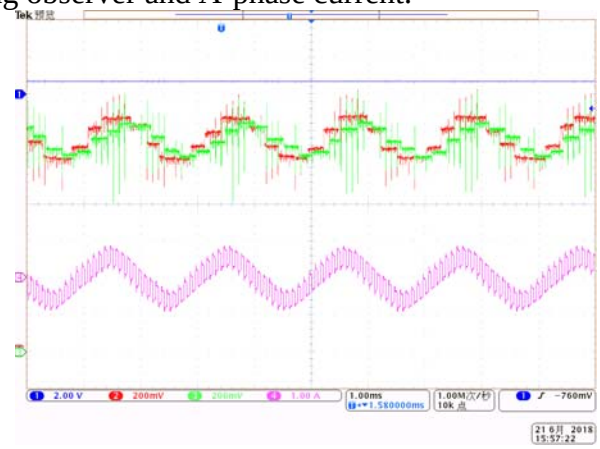

Figure 8. Waveforms of d–axis reference current and its actual one, phase A current and rotor position angle (500Hz)

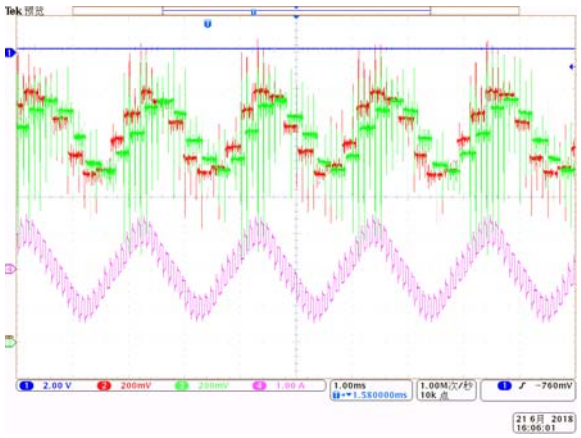

Figure 9. Waveforms of q–axis reference current and its actual one, phase A current and rotor position angle(500Hz)

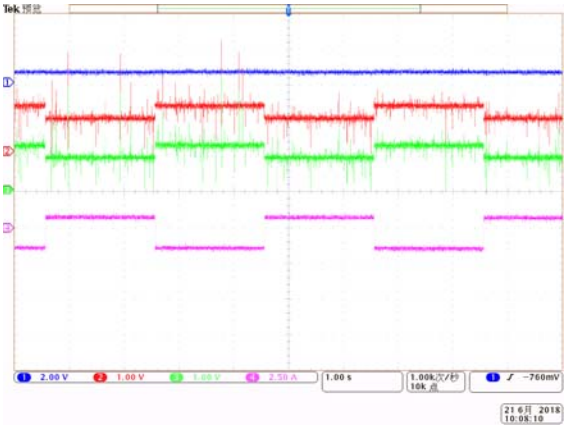

Figure 10. Waveforms of d–axis reference current and its actual one, A-phase current and rotor position angle (Square Wave reference case)

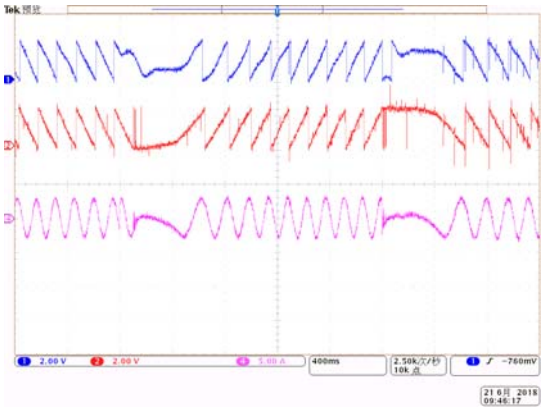

Figure 11. Waveforms operating at ± 100rpm and transition between each other with load (load torque 0.2Nm)

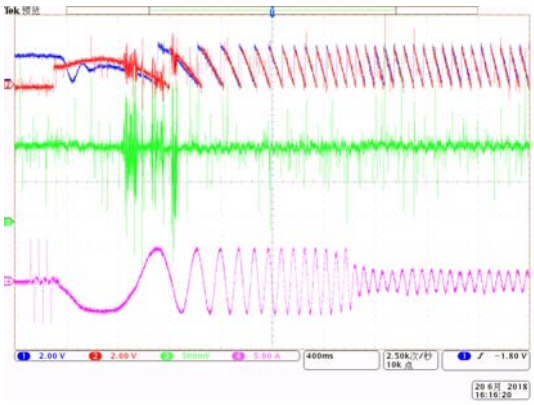

Figure 12. Waveforms of step response with rotor speed reference as -100rpm and load (load torque 0.3Nm)

Fig.12 is the waveforms when a desired step speed (-110rpm) is applied with load condition. The definition of waveforms from top to bottom in Fig.12 is real rotor position from encoder, the estimated rotor position from tracking observer, the estimated error of rotor position and A-phase current, in which 3 times variations of A-phase current for polarity judgment during starting process.

Since the proposed scheme of sensorless vector control only runs properly at zero and low- speed region, once the speed is over certain value, other strategies such as EMF based sensorless scheme, e.g., flux observer, should be changed over [3][5-6]. Experimental results of combination between the proposed scheme and stator-flux based observer are shown in Fig.13. The definition from top to bottom in Fig.13 is the real rotor position from encoder, the estimated rotor position from the proposed scheme, the rotor position from stator-flux based observer and A-phase current. When the rotor runs from zero speed to 200rpm, the proposed high-frequency injection scheme is adopted. While the rotor just runs between 200rpm and 400rpm, both the proposed and the stator-flux based observer act simultaneously. And effect of the proposed scheme becomes weaker, while that of the stator-flux based scheme becomes more and more important. Once the speed is over 400rpm, the proposed scheme stops and the stator-flux based observer works totally. From Fig.13 we can see that the proposed scheme can works well in wide speed ranges.

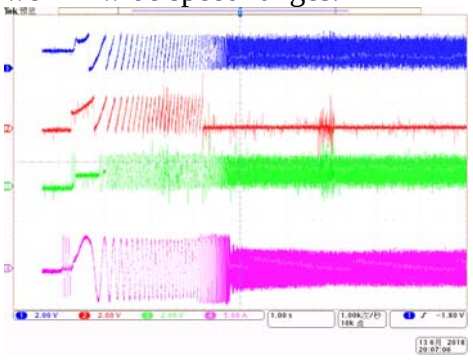

Figure 13. Waveforms of transition from high-frequency carrier injection to flux observer with load torque(n*=1500rpm, Tl = 0.3Nm)

Conclusions

This paper, based on a high-frequency square waveform injection method, presents a new scheme for realizing sensorless speed vector control system of SPMSM. Besides its capability for running stably at low- speed and switching between clockwise and counterclockwise, the proposed scheme also has following advantages:

- No additional noise exists from the high-frequency voltage injection, different from the high-frequency injection method at present.
- Bandwidth of the current-loop is not degraded due to application of modulation and demodulation. Thus, dynamic performance of original control system remains the same as that with encoder.
- Influence from dead-zone of inverter is eliminated. Therefore, the estimated accuracy for rotor position is ensured.

Acknowledgment

This work was supported by Foundation of grand Creative Engineering Project of Shandong Province, P. R. China, and funded project (2017CXGC0203).

References

[1] Dianguo Xu, Bo Wang, Guoqiang Zhang, Gaolin Wang, Yong Yu.”A review of sensorless control methods for AC motor drives.” CES Transactions on electrical machine and system,vol. 2(1), 2018, pp.104-115.

[2] Guoqiang Zhang, Gaolin Wang, Dianguo Xu. Saliency-based position

sensorless control methods for PMSM drives–a review [J]. Chinese Journal of Electrical Engineering, 2017, 3(2):14-23.

[3] Antti Piippo, Marko Hinkkanen, Jorma Luomi, Adaption of motor parameters in sensorless PMSM drives [J]. IEEE Transactions on Industry Applications, 2009, 45(1): 203-212.

[4] Zhong zhenfeng,Jin Mengjia,Shen Jianxin. Full speed range sensorless control of permanent magnet synchronous motor with phased PI regulator-based model reference adaptive system [J]. Proceeding of the CSEE, 2018, 38(4) : 1203-1211.

[5] Jingbo Liu, Thomas A. Nondahl, Peter B. Schmdit, Semyon Royak, Mark Harbaugh. Rotor position estimation for synchronous machine based on equivalent EMF [J]. IEEE Transactions on Industry Applications, 2011, 47(3): 1310-1318.

[6] Ion Boldea, Mihaela Paicu, Gheorghe-Daniel Andreescu. Active flux concept for motion sensorless unified AC drive[J]. IEEE Transactions on Power Electronics, 2008,23(5): 2612-2618.

[7] Liu J.M., Zhu Z. Q.,Sensorless control strategy by square-waveform high-frequency pulsating signal injection into stationary reference frame[J]. IEEE Transactions on Power Electronics, 2014, 2(2):171-180.

[8] Shao Junbo, Wang Hui, Huang Shoudao,Wu Xuan. A position sensorless control strategy of surfaced-mounted permanent-magnet synchronous motors for low-speed operation [J]. Proceeding of the CSEE, 2018,38(5):1534-1541.

[9] Ge Xie, Kaiyuan Lu, Sanjeet Kumar Dwivedi, Jesper Riber Rosholm, Frede Blaabjerg, Minimum-voltage vector injection method for sensorless control of PMSM for low-speed operation[J]. IEEE Transactions on Power Electronics, 2016, 31(2):1785-1794.

[10] Young-Doo Yoon, Seung-Ki Sul, Shinya Morimoto,Kozo Ide. High-Bandwidth sensorless Algorithm for AC Machine Based on Square-wave-type voltage injection [J]. IEEE Transactions on Industry Applications, 2011, 47(3): 1361-1370.

[11] Dong Kim, Yong Cheol Kwon, Seung-Ki Sul, jang-Hwan Kim, Rae-Sung Yu. Suppression of injection voltage disturbance for high-frequency square-wave injection sensorless drive with regulation of induced high- frequency current ripple [J]. IEEE Transactions on Industry Applications, 2016, 52(1): 302-312.

[12] Ronggang Ni, Dianguo Xu, Frede Blaabjerg,Kaiyuan Lu, Gaolin Wang, Guoqing Zhang, Square-wave voltage injection algorithm for PMSM position sensorless control with high robustness to voltage errors[J]. IEEE Transactions on Power Electronics, 2017,32(7):5425-5437.

[13] Wan Shan ming, WU Fang, Huang Sheng hua. Initial rotor position estimation of permanent magnet synchronous motor based on high frequency voltage signal injection method [J]. Proceeding of the CSEE, 2008, 28(33): 82-86.

[14] Hyunbae Kim, Kum-Kang Huh, Robert D. Lorenz, Thomas M.Jahns. A novel method for initial rotor position estimation for IPM synchronous machine drives [J]. IEEE Transactions on Industry Applications, 2004, 40(5): 1369-1377.

[15] Chuangang Wang, Longya Xu. A novel approach for sensorless control of PM machine down to zero speed without signal injection or special PWM technique [J]. IEEE Transactions on Power Electronics, 2004,19(6): 1601-1607.

[16] Joachim Holtz. Acquisition of position error and magnet polarity for sensorless control of PM synchronous machines [J]. IEEE Transactions on Industry Applications,2008,44(4):1172-1180.